Biomedical Signal Processing and Control 40 (2018) 263–274

Contents lists available at ScienceDirect

Biomedical Signal Processing and Control

journal homepage: www.elsevier.com/locate/bspc

A robust QRS complex detection using regular grammar and deterministic automata

Salah Hamdi*, Asma Ben Abdallah, Mohamed Hedi Bedoui

Laboratory of Technology and Medical Imaging (LTIM), Faculty of Medicine of Monastir (FMM), University of Monastir, Monastir, Tunisia

ARTICLE INFO

Article history:
Received 7 November 2016
Received in revised form 6 September 2017
Accepted 30 September 2017
Available online 12 October 2017

Keywords:
DFA
Grammar
ECG
QRS
R peak
RR
σRR
σQRS

ABSTRACT

A novel approach is proposed for medical analysis and clinical decision support of the Electrocardiogram (ECG) signals based on the deterministic finite automata (DFA) with the addition of some requirements. This paper proves regular grammar is effective in the extraction of QRS complex and interpretation of ECG signals. The DFA will be used to represent a normalized QRS complex as a sequence of negative and positive peaks. A QRS is considered as a set of adjacent peaks that satisfy certain criteria of standard deviation and duration. The proposed method is applied on several kinds of ECG signals collected from the standard MIT-BIH arrhythmia database. Several metrics are calculated including QRS durations, RR distances and peak amplitudes. Furthermore, σRR and σQRS metrics were added to quantify RR distances regularity and QRS durations, respectively. Regular grammar with the addition of some requirements and deterministic automata proved functional for both biomedical signals and ECG signal diagnosis. The suggested method provided a sensitivity rate of 99.74% and the positive predictivity rate of 99.86%. The algorithm was compared to other works in the literature and the quality performance detection was compared with several algorithms tested and validated on the MIT-BIH database. A head-to-head comparison in terms of sensitivity and CPU runtime was provided with the wavelet method.

1. Introduction

Understanding the medical signal information has been a fundamental issue in the field of biomedical signal processing. Several approaches have tried to overcome this difficulty using syntactic and grammatical methods. The syntactic methods can represent different lesions in medical signals such us ElectroEncephaloGraphy (EEG) and ElectroCardioGraphy (ECG) signals. Various ECG signal analysis methods, including the Support Vector Machine (SVM) [1–6], the fuzzy neural networks [7–10] and the wavelets [11–19], have been used. Sahambi et al. [20,21] used the first order derivative of the Gaussian function as a wavelet for the characterization of ECG beats. The author used the dyadic wavelet transform to detect and measure the different parts of a signal, especially the location of the beginning and end of the QRS complex. Sahambi et al. showed the robustness of the algorithm in the presence of a high frequency noise added to the signal. In [22], a dyadic wavelet transform was used to extract the characteristics of the ECG signal. The algorithm detected the QRS complex and the T wave, and then the P wave. Gramatikov et al. [23] focused on the morphology of the QRS complex and utilized the Morlet wavelet transform for the ECG recordings analysis in patients with left or right coronary stenosis.

The QRS complex detection is a key step to achieve an automatic analysis of ECG signals [24–28]. QRS complexes detection can be performed by a simple thresholding of the signal in terms of amplitude as the R peaks are generally larger than the other waves. Occasionally, the amplitude of the T wave is similar to that of the R peak. Indeed, this can cause errors in the final result and the detection rate. In addition, the R peak can sometimes have a variable morphology and low amplitude from one cardiac cycle to another. As a result, a good detection of the QRS complex is essential. This task requires a very adequate signal processing, taking into account the encountered difficulties. The evolution of the robustness of the digital processing software tools assures the design and implementation of the various versions of algorithms intended for the automatic detection of the QRS complexes. Therefore, QRS complex detection has been the target of many works and continues to be an axis of active research [29,30].

Several QRS-complex-research algorithms have been used based to a great extent on the proportionately high amount of QRS energy [31]. Most algorithms are based on the application of neural networks, hidden Markov model, syntactic methods, etc. [32–43]. However, they have been seldom used in low-cost computing applications. More details about the complex QRS detection techniques,

* Corresponding author.
E-mail address: hamdisalah@yahoo.fr (S. Hamdi).

https://doi.org/10.1016/j.bspc.2017.09.032
1746-8094/

comparing their effectiveness and their calculation complexities, can be found in the presence of noise. QRS detection algorithms are generally based on one of the temporal derivatives of methods, wavelets, filter banks and mathematical morphology [44–48]. Based on a literature review, the complex methods for detecting the QRS are discussed in the following sections. These approaches are robust and allow a high accuracy rate that exceeds 99%. Kohler et al. [49] presented a detailed study summarizing the different techniques for QRS detection. The above mentioned methods are sorted by categories with a comparison of their performance.

However, very few approaches were based on grammatical formalism [50]. Kokai et al. [51] used grammar to classify QRS complexes and distinguish between QRS and the non-QRS patterns. Panagiotis et al. [52] opted for a syntactic method aimed at ECG recognition and measurement of the associated parameters. Yet, these methods were very sensitive to noise. Several morphologies produced erroneous peaks and thus impeded the grammatical description of the signal. Moreover, the authors did not use grammar formalism during the extraction phase of the peaks. Peak recognition was carried out using another method regardless of grammar. Hamdi et al. [53] presented a context-free grammar to describe an entire ECG signal. Nevertheless, this could not represent all the various types of ECG signals. The author focused only on normal cases and the method was applied on short signal durations. Besides, the author compared his approach with the old techniques adopted by Holsinger [54] and Fraden and Neuman [55]. Hanieh et al. [56] proposed to detect atrial arrhythmia by a regular expression. The input signal is considered as a string where each character represents an ECG signal element. Different experiments on MIT-BIH arrhythmia database show the efficacy of the method compared with conventional approaches. However, this algorithm has a sensitivity rate below 96.3%

The syntactic approaches can represent the pattern structures efficiently and facilitate data retrieval by means of their structures. The main advantage of these methods is that the representation is conspicuous. The syntactic approaches can powerfully represent the pattern structures and therefore make information recovery easier. The input data seem to be a structured scene having a hierarchical order as grammar clearly represents hierarchical structures using non-terminal and terminal nodes. The syntactic approaches can describe a large set of complex patterns using small sets of simple primitives and grammatical rules. Besides, Gao et al. [57] affirmed that the use of grammar, compared to statistical methods, provides more flexibility in applications.

It is in this context that this work is put forward. The learning automata have been exploited to recognize rest phases, negative and positive peaks. The QRS complex has been described using deterministic automata. Several metrics were determined, namely the number of QRS complexes, the QRS durations, the RR distances, and the peak amplitudes. The proposed method is performing in terms of sensitivity rate, positive predictivity rate, R peak accuracy detection and CPU runtime.

The rest of the paper is organized as follows. Section 2 sheds the light on the material and the suggested method. Section 3 presents and discusses the results, and a comparative study provides several statistical methods in terms of sensitivity rates. A head-to-head comparison in terms of sensitivity and CPU runtime is provided with wavelet method. We conclude in Section 4.

2. Materials and methods

2.1. ECG signal presentation

The ECG is the measure of the electrical activity during the contraction of the heart. It is characterized by waves called P and T. The Q, R and S peaks form the QRS complex [58]. The potential difference between each electrode pair represents the electrical activity of the heart from several points of view where the sampling frequency is generally between 200 Hz and 500 Hz. In an ECG signal, the phenomena of contraction and relaxation of the myocardium are shown in the form of a sequence of superposed negative and positive deflections on a base line of zero potential that suits the absence of cardiac events.

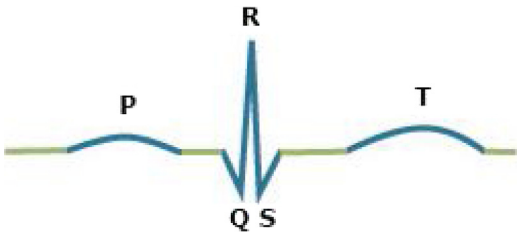

Fig. 1. One cardiac cycle of an ECG signal.

Fig. 1 represents one cardiac cycle of an ECG. The letters P, Q, R, S and T waves successively assign the ECG signal. The repolarization phase of the atria explains the QRS complex. When this pulse is much stronger than the first, the repolarization wave will become hidden. The QRS com-plex is the set of positive and negative deflections that are suitable for the contractions of both ventricles. It is often made up of three waves. First, the Q wave is the first negative deflection. Second, the R wave is the first positive deflection. Finally, the S wave is the second negative defec-tion following the R peak. The shape of the QRS complex is variable depending on the positions of the electrodes and also on the used derivations. The QRS represents the ventricular depolarization curve. All these three peaks are the QRS complex having durations between 0.06 and 0.1 s. In a resting state, heartbeat is between 60 and 80 beats per minute. An accelerated number of beats is called tachycardia. A slowdown in the number of beats is called bradycardia. An irregular heart rhythm is called an irregular rhythm. All such forms are basic forms of arrhythmia.

2.2. Method outline

Fig. 2 summarizes all the method's steps. The ECG is filtered, centralized and normalized. Then, the lexical analysis step recognizes the tokens including positive and negative peaks. A QRS complex is considered as a set of adjacent peaks which satisfy also certain criteria of standard deviation and duration. It is described by means of deterministic automata and regular expressions. Eventually, the analyzer determines the RR distances, the complex-QRS durations, the standard deviation of RR distances, the standard deviation of QRS durations, and a report is generated according to sampling frequency, time and amplitude values.

2.3. Preprocessing

An ECG signal S[n] is actually too noisy, hence some preprocessing phases are needed to reduce noise and then facilitate lexical analysis. The desirable pass-band is approximately 5–15 Hz [33] to reduce the influence of muscle noise, 60 Hz interference, base line wander, and T wave interference.

The following mathematical equations describe the different steps of the preprocessing phase. An example is displayed later in Fig. 3 where a normalized and centered ECG signal is filtered by a band-pass filter.

Step 1: Filtering the signal where H [n] is a 2nd order band-pass filter and the cutoff frequency is 5–15 Hz.

$$S1[n] = S[n] * H[n] \quad (1)$$

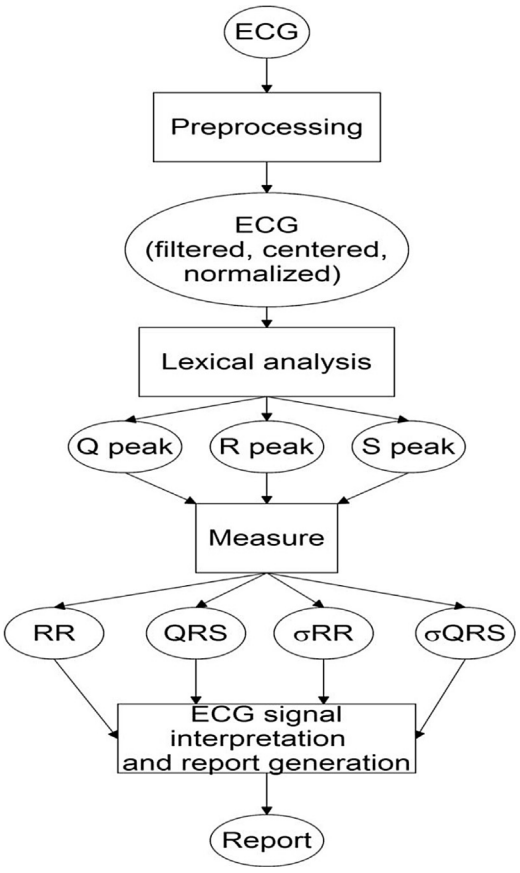

Fig. 2. An outline of the method.

Step 2: Centralizing the signal where the m parameter is the signal length.

$$S2[n] = S1[n] - \frac{\sum_{i=1}^{m} S1[i]}{m} \tag{2}$$

Step 3: Normalizing the signal amplitude:

$$S3[n] = \frac{S2[n] - Mean(S2[n])}{Max(S2[n] - Mean(S2[n]))} \tag{3}$$

Fig. 3 illustrates an example of a real ECG signal before and after preprocessing. Preprocessing reduced noise, centralized and normalized the signal.

2.4. Standard deviation and duration variation

Mathematically, a positive or negative peak must have a higher standard deviation σ greater than a threshold σ1 and a low duration Δ less than a threshold Δ1.

Given the sampling frequency *Fe*, a signal component is made up of a sequence of *n* normalized amplitudes {*a1, a2, . . ., an*}. The equations below calculate the standard deviation σ and the duration Δ is as follows:

$$\sigma = \sqrt{\sum_{i=1}^{n} \frac{\left(ai - \sum_{i=1}^{n} \frac{ai}{n}\right)^2}{n}} \tag{4}$$

$$\Delta = \frac{n}{Fe} \tag{5}$$

Fig. 4 plots the standard deviations variation of Q, R and S peaks as well as P and T waves. Both R and S peaks show very important standard deviations that are higher than 0.2. The Q peak has standard deviations higher than 0.1 whereas P and T waves have much lower values of standard deviations below 0.05. According to Fig. 4, starting at σ1 = 0.1, we can distinguish between the peaks and the waves.

Fig. 5 plots the duration variation of Q, R and S peaks as well as P and T waves. The peaks Q, R and S show very small durations lower than 0.1 s. while both P and T waves have higher values of durations more than 0.1 s. According to Fig. 5, starting at Δ1 = 0.1 s, we can distinguish between the peaks and the waves. A QRS complex is actually considered as a set of adjacent peaks that meet the requirements of standard deviation and duration.

2.5. Lexical analysis of the ECG signal

In this section, the signal amplitude is considered as a sequence of values belonging to the interval [−1, 1]. The normalized amplitude is referred to as a sequence of almost nil, negative and positive values; i.e., the signal is considered as a language where the QRS complex represents a suite of words. Therefore, the alphabet $\sum$ = {0,1,2,3,4,5,6,7,8,9, −, .} is enough to represent a normalized amplitude belonging to the interval [−1, 1]. Then, the regular expressions perform the lexical analysis of the signal to represent the rest phase, the positive peak and the negative peak, and make up the QRS complex.

Based on an alphabet Σ, a deterministic finite automaton, referred to as DFA, is a quadruple (Q, δ, i, F) where:

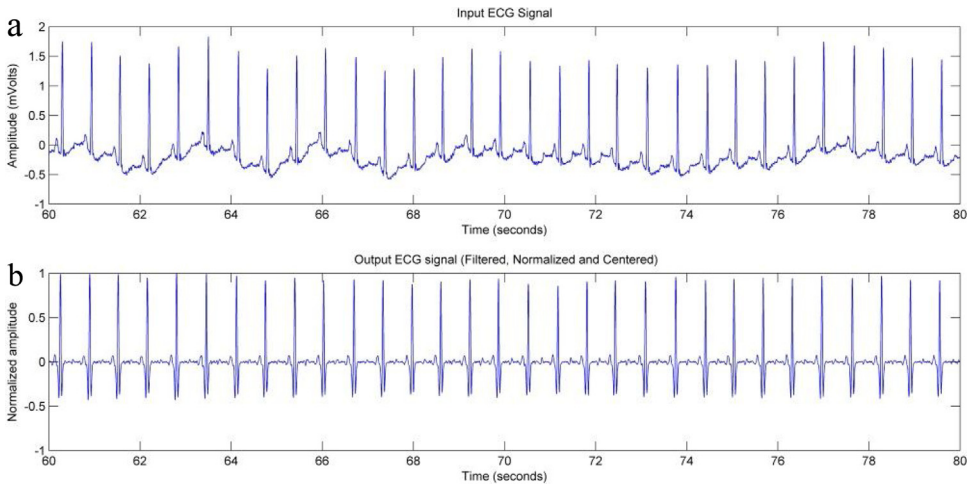

Fig. 3. (a) An input ECG signal before preprocessing; (b) The output signal after preprocessing.

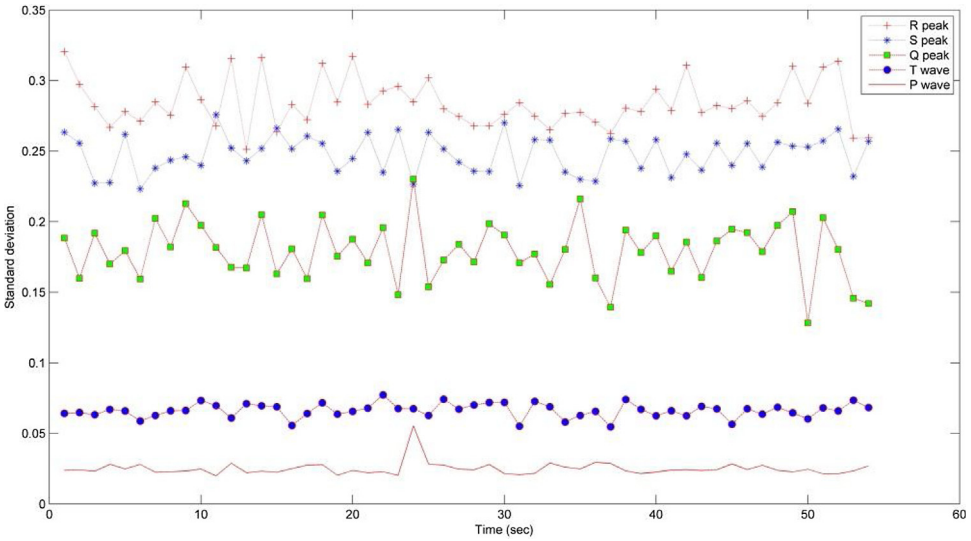

Fig. 4. Peak and wave standard deviation.

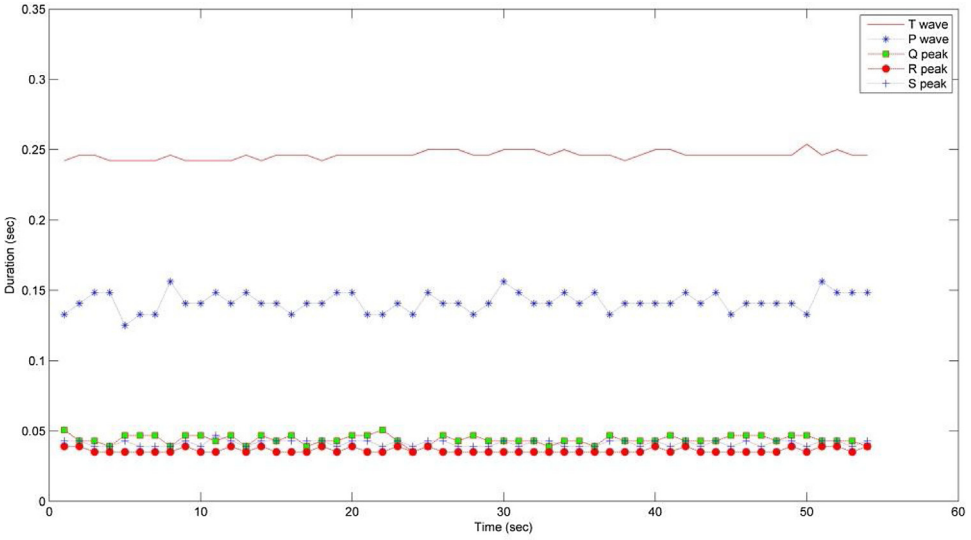

Fig. 5. Peak and wave duration.

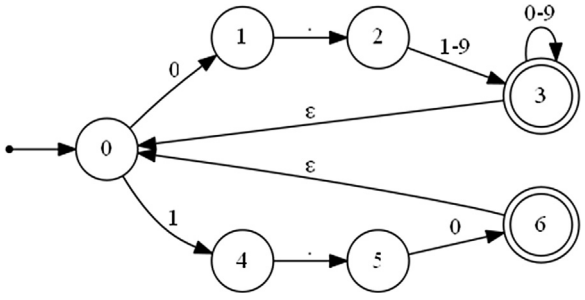

Fig. 6. A DFA illustrating a normalized positive peak (R).

- Q: a finite set of states.
- δ: a transition function Q × Σ in Q.
- i: a symbol of Σ alphabet.
- F: the final states; F ⊆ Q.
- q0: the start state; q0 ∈ Q.

The following DFA (Fig. 6) and the regular expression describe a normalized positive peak where the '€' character is an empty word having zero length, '*' means 'zero or more times', '+' means 'one or more times', and '?' means 'zero or one time':

$$R = \{0[1\text{–}9].[0\text{–}9] * |1.0\} + \tag{6}$$

$$\sigma R > \sigma 1 \tag{7}$$

$$\Delta R < \Delta 1 \tag{8}$$

The start sate q0 = {0}.
The finite set of states Q = {0,1,2,3,4,5,6}.
The final set of states F = {3,6}.
The transition functions are:
δ(0,0) = 1 δ(1,.)=2 δ(2,1-9) = 3 δ(3,0-9) = 3
δ(3,ε) = 0 δ(0,1) = 4 δ (4, .) = 5 δ (5,0) = 6
δ (6,ε) = 0

Fig. 7 and the regular expression below show the DFA describing a normalized negative peak:

$$Q = \{-0[1\text{–}9].[0\text{–}9] * |-1.0\} + \tag{9}$$

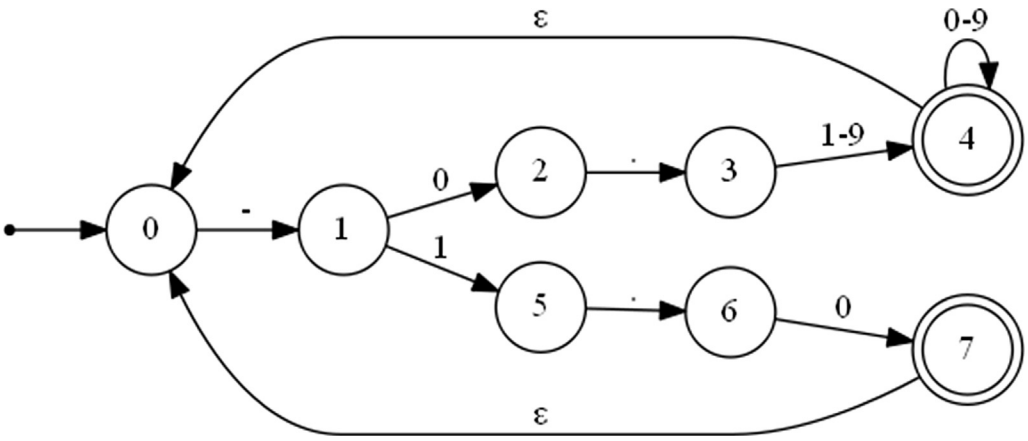

Fig. 7. A DFA illustrating a normalized negative peak (Q or S).

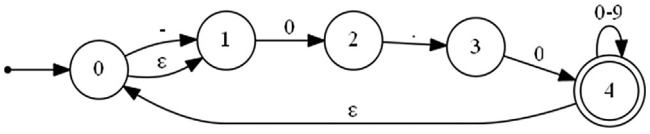

Fig. 8. A DFA illustrating a normalized and short rest phase separating the peak.

$$\sigma Q > \frac{\sigma 1}{2} \tag{10}$$

$$\Delta Q < \Delta 1 \tag{11}$$

$$S = \{\text{-}0[1\text{–}9].[0\text{–}9]*|\text{-}1.0\}+ \tag{12}$$

$$\sigma S > \sigma 1 \tag{13}$$

$$\Delta S < \Delta 1 \tag{14}$$

The start sate q0 = {0}.
The finite set of states Q = {0,1,2,3,4,5,6,7}.
The final set of states F = {4,7}.
The transition functions are:
δ(0,-) = 1 δ(1,0) = 2 δ(2,.) = 3 δ(3,1-9) = 4
δ(4,0-9) = 4 δ(4,ε) = 0 δ(1,1) = 5 δ (5,.) = 6
δ (6,0) = 7 δ (7, ε) = 0

Fig. 8 and the regular expression below show a normalized and short rest phase separating the peaks:

The start sate q0 = {0}.
The finite set of states Q = {0,1,2,3,4}.
The final state F = {4}.
The transition functions are:
δ(0,-) = 1 δ(0,ε) = 1 δ(1,0) = 2 δ(2,.) = 3 δ(3,0) = 4
δ(4,0-9) = 4 δ(4,ε) = 0

$$rest = \{\{\text{-}\}?0.0[0\text{–}9]*\}+ \tag{15}$$

$$\Delta rest < \frac{\Delta 1}{2} \tag{16}$$

Fig. 9 and the regular expression below describe a normalized QRS complex. Please note that the regular expression and the deterministic automaton below presume that the Q peaks and the rest phases may be absent.

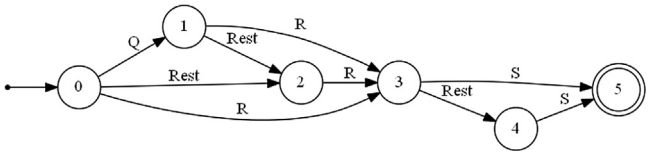

Fig. 9. A simplified DFA representing an entire normalized QRS complex.

$$QRS = \{Q\}?\{rest\}?\{R\}\{rest\}?\{S\} \tag{17}$$

The start sate q0 = {0}.
The finite set of states Q = {0,1,2,3,,,27,28}.
The final set of states F = {27,28}.
The transition functions are:
δ(0,.) = 1 δ(1,0) = 2 δ(2,.) = 3 δ(3,1-9) = 4
δ(4,0-9) = 4 δ(4,ε) = 6 δ(1,1) = 5 δ(4,ε) = 0
δ(5,ε) = 6 δ(5,ε) = 0 δ(6,0) = 7 δ(7,.) = 8
δ(8,0) = 9 δ(6,.) = 10 δ(10,0) = 11 δ(11,.) = 8
δ(9,0-9) = 9 δ(9,ε) = 6 δ(6,ε) = 12 δ(0,ε) = 12
δ(9,ε) = 12 δ(12,0) = 13 δ(13,.) = 14 δ(14,1-9) = 15
δ(15,ε) = 17 δ(15,ε) = 12 δ(12,1) = 16 δ(16,ε) = 12
δ(16,ε) = 17 δ(17,0) = 18 δ(18,.) = 19 δ(19,0) = 20
δ(20,0-9) = 20 δ(17,.) = 21 δ(21,0) = 22 δ(22,.) = 19
δ(20,ε) = 17 δ(17,ε) = 23 δ(20,ε) = 23 δ(23,.) = 24
δ(24,0) = 25 δ(25,.) = 26 δ(26,1-9) = 27 δ(27,ε) = 23
δ(27,0-9) = 27 δ(24,1) = 28 δ(28,ε) = 23

The transition functions above and the associate DFA are simplified into the following automaton:

The start sate q0 = {0}.
The finite set of states Q = {0,1,2,3,4,5}.
The final set of states F = {5}.
The transition functions are:
δ(0,Q) = 1 δ(0,Rest) = 2 δ(0,R) = 3
δ(1,Rest) = 2 δ(1,R) = 3 δ(2,R) = 3
δ(3,Rest) = 4 δ(3,S) = 5 δ(4,S) = 5

In the following section, the method described above will be applied on the standard MIT-BIH database. The MIT-BIH arrhythmia database contains 48 excerpts of two-channel ambulatory ECG recordings. A total of 23 recordings were randomly chosen from a set of 4000. 24-h ambulatory ECG recordings were collected from a mixed population of patients (about 60%) and outpatients (about 40%). The sampling frequency was 360 Hz, the gain was 200 and the base was 1024mv.

The True Positive (TP), the False Positive (FP), the False Negative (FN), Sensitivity (Se), and Positive Predictivity (+P) metrics will be computed where:

TP: the correctly detected QRS.
FP: the incorrectly detected QRS.
FN: the incorrectly rejected QRS.

$$Sensitivity\,(\%) = \frac{TP}{TP + FN} * 100 \tag{18}$$

$$PositivePredictivity\,(\%) = \frac{TP}{TP + FP} * 100 \tag{19}$$

Moreover, two metrics are suggested: σRR and σQRS to quantify the regularity of n RR distances and $(n+1)$ QRS durations respectively.

$$\sigma RR = \sqrt{\sum_{i=1}^{n} \frac{\left(RRi - \sum_{i=1}^{n} \frac{RRi}{n}\right)^2}{n}} \tag{20}$$

$$\sigma QRS = \sqrt{\sum_{i=1}^{n+1} \frac{\left(QRSi - \sum_{i=1}^{n+1} \frac{QRSi}{n+1}\right)^2}{n+1}} \tag{21}$$

An almost nil σRR means that all the RR distances are regular. But, a σRR more than 0.1 means that the obtained values of the RR distances are irregular. Uniformly, an almost nil σQRS means that all the QRS durations are regular. Nevertheless, a σQRS more than 0.1 implies the obtained values of the QRS durations are irregular.

3. Results and discussion

3.1. Results

Table 1 demonstrates an application of the proposed method on several kinds of ECG signals issued from the MIT-BIH arrhythmia database in order to extract the QRS complex. For an input signal, several parameters were determined, such as the number of the QRS, the average RR distance $\overline{RR}$ and the average QRS duration $\overline{QRS}$, σRR, σQRS, TP, FP, FN, Se, and +P.

Practically, the average sensitivity (Se) rate of the proposed method is 99.74% and the average positive predictivity (+P) rate is 99.86%. The average RR distance is about 0.82 s and the QRS duration is about 0.07 s. Some records such as 108 and 119 represent an irregular beat rate. In fact σRR is 0.21 and 0.25 respectively.

Figs. 10 and 11 show an application on a portion of record 119 representing an irregular beat rate. The various indicators of the signal (RR distance; QRS complex duration; Q, R and S amplitudes) are displayed. The average value of RR and QRS are 0.91 s and 0.06 s respectively. However, the RR distances are irregular. In fact σRR = 0.20. This more or less high value proves that the RR distance is not stable.

The QRS complexes have normal durations of less than 0.1 s. In addition, they are regular. Indeed σQRS=0.02. This low value shows the QRS duration is stable.

The R peak amplitude is often about 2mv except that in three cases it decreases to 1mv whereas Q and S amplitudes are always about −1mv.

Figs. 12 and 13 illustrate an application on recording portion 100 representing a regular beat rate. Principally, the average value of RR and QRS are 0.81 s and 0.05 s respectively. Besides, the RR distances are regular and σRR=0.05. This low value shows that the RR distance is stable. Also σQRS=0.01; this almost nil value indicates that the QRS duration is stable.

The R peak amplitude is often about 1mv whereas Q and S amplitudes are about −0.5mv.

3.2. Noise sensitivity

Table 2 shows the variation of sensitivity (Se) and positive predictivity (+P) rates according to Signal-to-Noise Ratio (SNR). The method is applied on different ECG recordings 100, 101, 102, 103 and 105 collected from the MIT-BIH database.

According to Table 2, when the SNR values are greater than 40 dB, the method provides higher sensitivity and positive predictivity values that exceed 99%. When greater than 30 dB, the sensitivity and positive predictivity values exceed 97%. However, with SNR values lower than 25 dB, the sensitivity and positive predictivity values decrease up to 90%.

Fig. 15 shows the variation of average sensitivity (Se) and positive predictivity (+P) rates depending on the SNR. Usually, the sensitivity and the positive predictivity become increasingly important where SNR values are greater than 30 dB. For the SNR values less than 25 dB, the method offers low rates that are less than 90%.

3.3. R peak detection accuracy

In this section, we studied the method performance in terms of accuracy of R peaks detection and RR distance calculation. For this, the exact time of the first and the second R peaks from the recording 100 to recordings 110 are determined. Thus, for each peak, the accuracy value was determined. According to the values presented in Table 3, the accuracy values are greatly reduced and vary between 0.000 s and 0.010 s. On average, the accuracy value of R peak detection is 0.002 s while the accuracy value of RR distance calculation is 0.003 s. Fig. 14 illustrates the variation of R peak detection accuracy.

3.4. Head-to-head comparison

In this section, the method described above is applied on several real ECG signals representing different patients and collected from the Functional Exploration and Nervous System Department at Sahloul Hospital in Tunisia.

For all the input signals, the Q, R and S peaks, the RR distances, the QRS complex, are detected. Moreover, a head-to-head comparison with the wavelet method [19] is provided in terms of sensitivity (Se) rates.

Table 4 shows an application on several real ECG signals to extract the QRS where:

TP: the correctly identified QRS;

FP: the incorrectly identified QRS;

FN: the incorrectly rejected QRS.

The average sensitivity rate of the proposed method is 99.42% and the average sensitivity rate of wavelet method [19] is 98.50%.

Table 5 demonstrates several applications on very long ECG signals representing different patients in order to extract QRS and measure the average values of the RR distances and the QRS durations. Moreover, a comparative study with the wavelet method [19] in terms of execution-time process was conducted. Please note that the used machine has the following characteristics: Core (TM) i7-2600 CPU, frequency=3.40GHZ and RAM=4GB.

The average RR distance is about 0.671 s. The QRS duration is about 0.101 s. Moreover, the execution time of the proposed method is about 66.04 s on average whereas the wavelet method [19] shows 69.96 s.

3.5. Discussion

To situate our method in relation to taking into account other works in the literature, the quality performance detection was compared with several approaches that were tested and validated on the same MIT-BIH data base in terms of sensitivity rates. They vary and each one is based on an appropriate technique [34,40,41,48,59–67].

Based on the results presented in Table 6, all these algorithms have good QRS complex detection capacity with sensitivity rates that exceed 99%. Similarly, the proposed method provides satisfactory and competitive results with 99.74% sensitivity and can be considered a powerful tool for the detection of the QRS complex in the ECG signal.

Table 1
Application on the MIT-BIH standard database: extraction of QRS complex, sensitivity and calculation of precision rates.

Record	Record length (sec)	Real number of QRS	TP	FN	FP	Se (%)	+P (%)	$\overline{RR}$(sec)	σRR	$\overline{QRS}$(sec)	σQRS
100	1805	2273	2272	1	0	99.96	100.00	0.79	0.05	0.05	0.00
101	1805	1865	1864	1	0	99.95	100.00	0.96	0.07	0.06	0.00
102	1805	2187	2183	4	2	99.82	99.91	0.83	0.09	0.14	0.01
103	1805	2084	2082	2	2	99.90	99.90	0.86	0.05	0.05	0.00
104	1805	2230	2211	19	24	99.15	98.93	0.81	0.08	0.04	0.04
105	1805	2572	2571	1	0	99.96	100.00	0.70	0.11	0.07	0.00
106	60	67	67	0	0	100.00	100.00	0.88	0.09	0.06	0.00
107	60	70	70	0	2	100.00	97.22	0.82	0.12	0.12	0.02
108	1805	1763	1761	2	0	99.89	100.00	1.02	0.21	0.09	0.08
109	1805	2532	2526	6	2	99.76	99.92	0.71	0.05	0.09	0.00
111	60	69	69	0	0	100.00	100.00	0.89	0.15	0.05	0.01
112	1805	2539	2537	2	6	99.92	99.76	0.71	0.03	0.06	0.00
113	1805	1794	1794	0	1	100.00	99.94	1.00	0.09	0.05	0.00
114	60	54	54	0	0	100.00	100.00	1.10	0.04	0.03	0.00
115	1805	1953	1953	0	0	100.00	100.00	0.92	0.08	0.05	0.00
116	60	78	78	0	0	100.00	100.00	0.76	0.01	0.06	0.00
117	1805	1535	1534	1	1	99.93	99.93	1.17	0.05	0.06	0.00
118	1805	2275	2275	0	12	100.00	99.48	0.78	0.10	0.07	0.00
119	1805	1987	1987	0	0	100.00	100.00	0.90	0.25	0.07	0.02
121	1805	1863	1861	2	3	99.89	99.84	0.96	0.09	0.08	0.00
122	1805	2476	2475	1	2	99.96	99.92	0.72	0.04	0.07	0.00
123	1805	1518	1517	1	4	99.93	99.74	1.18	0.12	0.06	0.00
124	60	49	49	0	0	100.00	100.00	1.21	0.02	0.07	0.01
200	60	87	87	0	0	100.00	100.00	0.72	0.40	0.09	0.01
201	60	90	90	0	0	100.00	100.00	0.66	0.13	0.06	0.00
202	1805	2136	2111	25	0	98.83	100.00	0.85	0.30	0.07	0.00
203	60	97	97	0	0	100.00	100.00	0.61	0.24	0.08	0.01
205	60	89	89	0	0	100.00	100.00	0.66	0.01	0.05	0.00
207	1805	1862	1859	3	0	99.84	100.00	0.96	0.21	0.07	0.09
208	60	87	87	0	0	100.00	100.00	0.69	0.26	0.07	0.02
209	1805	3004	3002	2	7	99.93	99.77	0.59	0.08	0.05	0.00
210	1805	2647	2606	41	9	98.45	99.66	0.69	0.13	0.07	0.01
212	1805	2748	2748	0	5	100.00	99.82	0.65	0.04	0.06	0.00
213	1805	3251	3243	8	2	99.75	99.94	0.55	0.04	0.06	0.01
214	1805	2262	2229	33	0	98.54	100.00	0.81	0.22	0.07	0.00
215	1805	3363	3337	26	0	99.23	100.00	0.54	0.09	0.06	0.00
217	1805	2208	2206	2	0	99.91	100.00	0.88	0.25	0.10	0.01
219	1805	2154	2152	2	0	99.91	100.00	0.83	0.22	0.06	0.00
220	1805	2048	2047	1	4	99.95	99.80	0.88	0.09	0.05	0.00
221	1805	2427	2400	27	0	98.89	100.00	0.75	0.20	0.06	0.01
222	60	75	75	0	0	100.00	100.00	0.81	0.12	0.05	0.00
223	60	80	80	0	0	100.00	100.00	0.75	0.08	0.07	0.00
228	60	68	68	0	0	100.00	100.00	0.86	0.27	0.07	0.01
230	1805	2256	2219	37	0	98.36	100.00	0.81	0.18	0.06	0.00
231	60	63	63	0	0	100.00	100.00	0.94	0.11	0.06	0.00
232	1805	1780	1747	33	4	98.15	99.77	1.03	0.65	0.06	0.00
233	60	94	94	0	0	100.00	100.00	0.58	0.13	0.07	0.01
234	1805	2753	2752	1	0	99.96	100.00	0.65	0.03	0.06	0.00
Total	58720	73562	73278	284	92	99.74	99.86	0.82	0.13	0.07	0.01

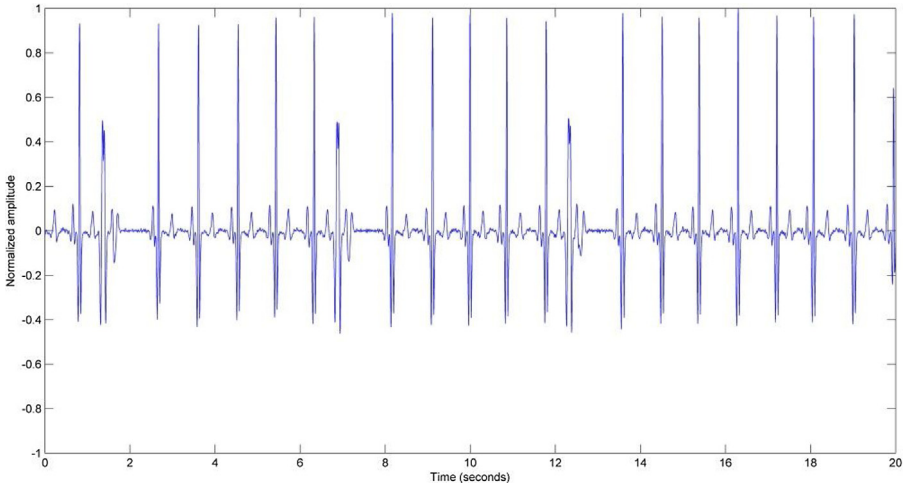

Fig. 10. A portion of a normalized recording 119 representing an irregular beat rate.

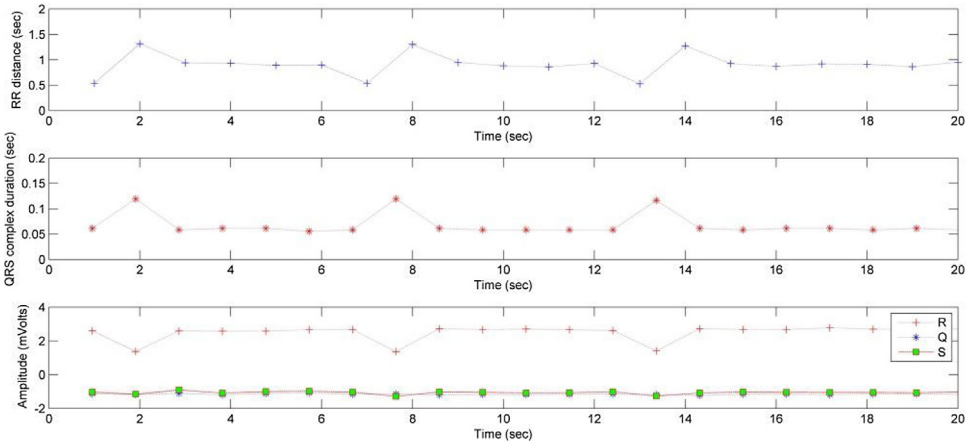

Fig. 11. (a) RR distances variation: $\overline{RR}$ = 0.91 s, σRR=0.20; (b) QRS durations variation: $\overline{QRS}$=0.06 s, σQRS=0.02; (c) Peaks amplitudes variation.

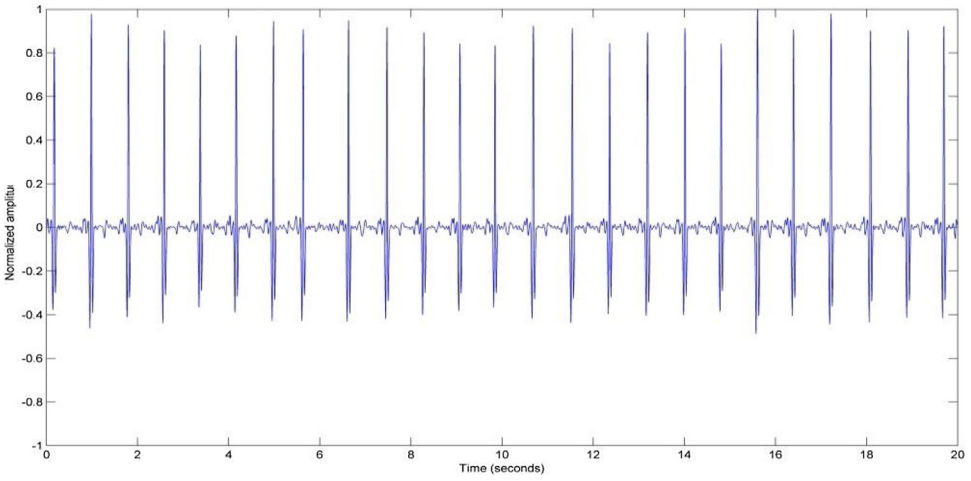

Fig. 12. A portion of a normalized recording 100 representing a regular beat rate.

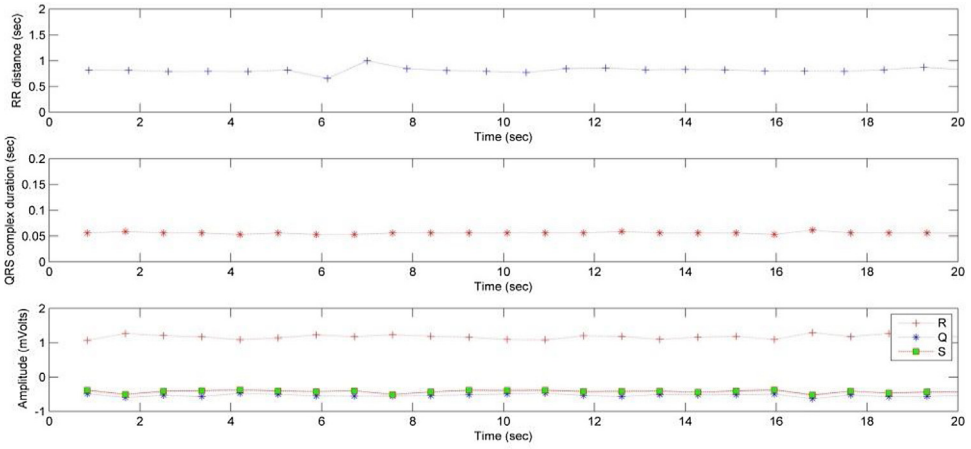

Fig. 13. (a) RR distances variation: $\overline{RR}$ = 0.81 s, σRR = 0.05; (b) QRS durations variation: $\overline{QRS}$ = 0.05 s, σQRS = 0.01; (c) Peaks amplitudes variation.

The suggested approach was tested using entire recordings from the MIT-BIH Arrhythmia database and from the Functional Exploration and Nervous System Department at Sahloul Hospital in Tunisia. From this database, a set of ECG waveform signals containing mechanical and electrical artifacts were chosen to test the performance of the new algorithm. A beat-by-beat comparison was performed and the results were shown in Tables 1 and 4. A false negative (FN) occurs when the algorithm fails to detect a true QRS and a false positive (FP) represents a false QRS detection. A true positive (TP) is the total number of QRS correctly located by the detector. Sensitivity (Se) and positive prediction (+P) were calculated.

Furthermore, the method shows a good performance for signals with noise even in the presence of pronounced muscular noise and baseline artifacts and the results are shown in Table 2. The accuracy of the proposed method on R peak time detection and RR distance calculation is given in Table 3. A head-to-head compari-

Table 2
Variation of sensitivity and positive predictivity rates.

Record	SNR (dB)	90	80	70	60	50	40	30	25	20
100	Se (%)	99.96	99.96	99.96	99.96	99.96	99.96	99.96	93.27	55.52
	+P (%)	100.0	100.0	100.0	100.0	100.0	100.0	99.91	83.73	57.52
101	Se (%)	99.95	99.95	99.95	99.95	99.95	99.95	99.79	95.28	48.04
	+P (%)	100.0	100.0	100.0	100.0	100.0	100.0	99.95	84.86	39.54
102	Se (%)	99.82	99.82	99.82	99.82	99.82	97.49	91.13	83.36	43.80
	+P (%)	99.91	99.91	99.91	99.91	99.91	96.22	88.90	83.51	40.47
103	Se (%)	99.90	99.90	99.90	99.90	99.90	99.90	99.86	97.46	54.89
	+P (%)	99.90	99.90	99.90	99.90	99.90	99.90	99.90	95.85	45.52
105	Se (%)	99.96	99.96	99.96	99.96	99.96	98.41	97.51	93.58	53.30
	+P (%)	100.0	100.0	100.0	100.0	100.0	99.10	99.09	95.90	61.01
Total	Se (%)	99.92	99.92	99.92	99.92	99.92	99.14	97.65	92.59	51.11
	+P (%)	99.97	99.97	99.97	99.97	99.97	99.20	97.95	88.12	47.27

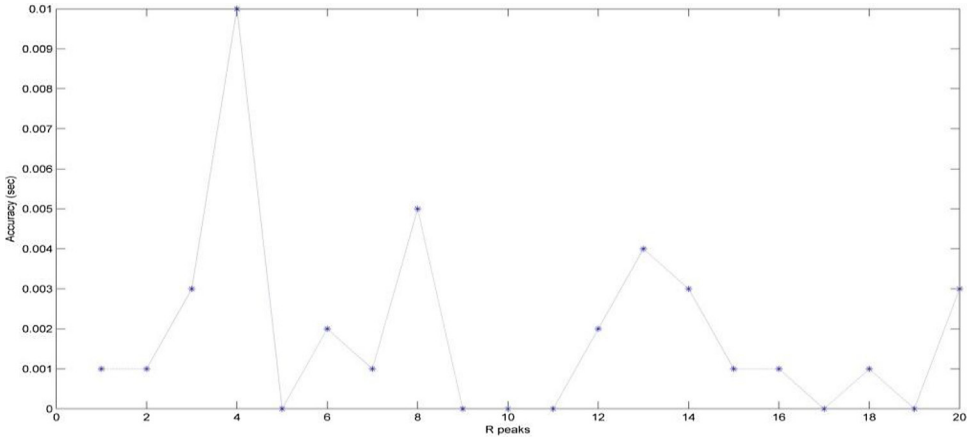

Fig. 14. Accuracy variation of R peak detection.

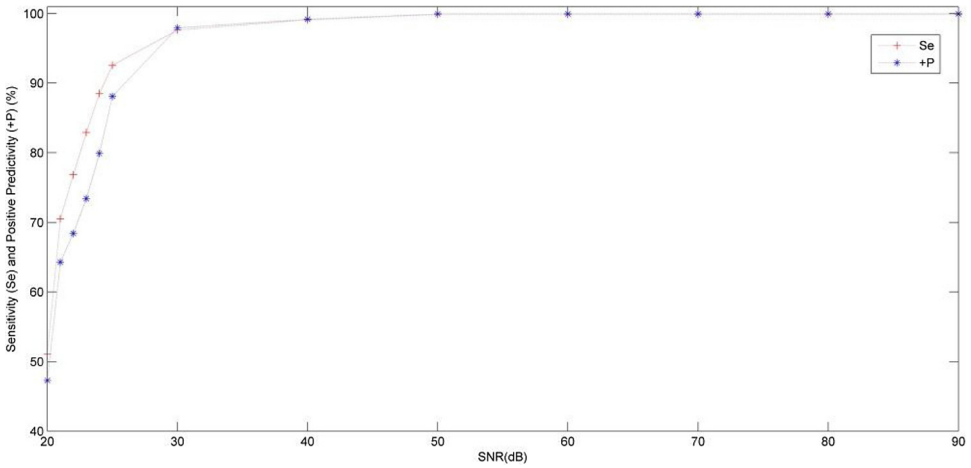

Fig. 15. Average sensitivity (Se) and positive predictivity (+P) variation according to SNR.

son with wavelet method was presented in Tables 4 and 5 in terms of Sensitivity (Se) and CPU runtime. The reliability of the proposed detector compares very favorably with published results for other QRS detectors and the results were given in Table 6.

4. Conclusion

In this paper, the DFA proved useful for the recognition of the QRS complexes and the interpretation of the ECG signals. A QRS complex is considered as a set of adjacent peaks that meet certain criteria of standard deviation and duration. This method recognizes the QRS complex in an ECG waveform. The QRS complex was described using deterministic finite automata and regular expressions. For an input signal, all the various indicators such as the complex-QRS durations, the RR distances, the standard deviation of RR distances, and the standard deviation of QRS durations next to Q, R and S amplitudes, were deduced. Moreover, σRR and σQRS parameters were added to quantify the regularity of RR distances and QRS durations, respectively. The proposed method was performed in terms of sensitivity and positive predictivity rates, R peak detection accuracy, RR distance accuracy and CPU runtime.

The present approach affirmed that, compared with statistical methods, the use of grammar can represent the QRS structures efficiently and therefore facilitate data retrieval. The QRS complex

Table 3
Accuracy of the proposed method on R peak time detection and RR distance calculation.

Record	R peak order	Exact R peak time (sec)	R peak time (sec)	Accuracy (sec)	Exact RR disatnce (sec)	RR distance (sec)	Accuracy (sec)
100	1	0.171	0.172	0.001	–	–	–
	2	0.985	0.986	0.001	0.814	0.814	0.000
101	1	0.189	0.186	0.003	–	–	–
	2	1.060	1.050	0.010	0.871	0.864	0.007
102	1	0.269	0.269	0.000	–	–	–
	2	1.090	1.088	0.002	0.821	0.819	0.002
103	1	0.693	0.694	0.001	–	–	–
	2	1.56	1.555	0.005	0.867	0.861	0.006
105	1	0.502	0.502	0.000	–	–	–
	2	1.230	1.230	0.000	0.728	0.728	0.000
106	1	0.933	0.933	0.000	–	–	–
	2	1.970	1.972	0.002	1.037	1.039	0.002
107	1	0.712	0.708	0.004	–	–	–
	2	1.530	1.533	0.003	0.818	0.825	0.007
108	1	0.140	0.141	0.001	–	–	–
	2	0.978	0.977	0.001	0.838	0.836	0.002
109	1	0.261	0.261	0.000	–	–	–
	2	0.906	0.905	0.001	0.645	0.644	0.001
110	1	0.507	0.507	0.000	–	–	–
	2	1.320	1.317	0.003	0.813	0.810	0.003
Average				0.002	–	–	0.003

Table 4
A Head-to-head performance comparison for QRS detection with wavelet method [19] in term of sensitivity rate.

ECG	Signal length (sec)	Real number of QRS	TP	FP	FN	Se (%)	Se using wavelet [19] (%)
ECG8	60	55	55	0	0	100.00	100.00
ECG9	90	87	87	1	0	100.00	96.55
ECG10	120	116	116	1	0	100.00	99.13
ECG11	150	145	144	1	1	99.31	96.55
ECG12	180	173	171	1	2	98.84	98.26
ECG13	210	202	201	2	1	99.50	97.52
ECG14	240	231	228	0	3	98.70	98.26
ECG15	270	260	258	0	2	99.23	98.07
ECG16	300	289	287	4	2	99.31	100.00
ECG17	400	391	388	5	3	99.23	99.74
ECG18	500	488	485	5	3	99.39	98.61
ECG19	600	585	582	5	3	99.49	99.31
Total	3120	3022	3002	25	20	99.42	98.50

Table 5
A Head-to-head performance comparison for QRS detection with wavelet method [19] in term of CPU runtime.

ECG	Signal length (hour)	Detected QRS	$\overline{RR}$ (sec)	$\overline{QRS}$ (sec)	CPU runtime (sec)	CPU runtime using wavelet [19] (sec)
ECG30	1	4836	0.743	0.101	11.26	14.05
ECG31	2	9969	0.721	0.100	23.24	29.91
ECG32	3	16465	0.655	0.104	37.28	43.14
ECG33	4	22037	0.653	0.103	54.46	58.37
ECG34	5	27357	0.657	0.102	72.36	74.09
ECG35	6	33127	0.651	0.101	90.87	92.57
ECG36	7	38728	0.650	0.101	109.78	112.84
ECG37	8	45019	0.639	0.101	129.08	134.71
Total	36	197538	0.671	0.102	66.04	69.96

Table 6
Comparison of performance of several QRS detection algorithms in the literature.

Method	Description	Sensitivity rate (%)
Pan et al. [33]	Derivative approach and analyzing the slope	99.30
Szu et al. [39]	Neural network and adaptive filtering	99.50
Sai et al. [40]	Euclidean distance metric and KNN algorithm	99.81
Ben et al. [47]	Discrete wavelet decomposition and energy calculation	99.39
Ham et al. [59]	Derivative approach and optimized process of rule decision	99.46
Cho et al. [60]	Multi wavelet packet decomposition	99.14
Had et al. [61]	Empirical modal decomposition (EMD)	99.92
Chr et al. [62]	Adaptive thresholding	99.65
Gha et al. [63]	Mathematical model and continuous wavelet transform (CWT)	99.91
Kry et al. [64]	Recursive temporal prediction	99.00
Meh et al. [65]	Approach based on Support Vector Machine	99.75
Gri et al. [66]	Duration and energy transformation	99.26
Tra et al. [67]	Mathematical morphology	99.38
The suggested approach	Regular grammar, standard deviation and duration calculation	99.74

seems to be a structured scene having a hierarchical order as grammar clearly can represents hierarchical structures and describe a large set of ECG signals.

References

[1] T. Ince, S. Kiranyaz, M. Gabbouj, A generic and robust system for automated patient-specific classification of ECG signals, IEEE Trans. Biomed. Eng. 56 (2009) 1415–1426, http://dx.doi.org/10.1109/TBME.2009.2013934.

[2] N. Ghoggali, F. Melgani, Y. Bazi, A multiobjective genetic SVM approach for classification problems with limited training samples, IEEE Trans. Geosci. Remote Sens. 47 (2009) 1707–1718, http://dx.doi.org/10.1109/TGRS.2008.2007128.

[3] A.H. Khandoker, M. Palaniswami, C.K. Karmakar, Support vector machines for automated recognition of obstructive sleep apnea syndrome from ECG recordings, IEEE Trans. Inf. Technol. Biomed. 13 (2009) 37–48, http://dx.doi.org/10.1109/TITB.2008.2004495.

[4] F. Melgani, Y. Bazi, Classification of electrocardiogram signals with support vector machines and particle swarm optimization, IEEE Trans. Inf. Technol. Biomed. 12 (2008) 667–677, http://dx.doi.org/10.1109/TITB.2008.923147.

[5] A. Kampouraki, G. Manis, C. Nikou, Heartbeat time series classification with support vector machines, IEEE Trans. Inf. Technol. Biomed. 13 (2009) 512–518, http://dx.doi.org/10.1109/TITB.2008.2003323.

[6] Y. Zhu, SVM classification algorithm in ECG classification, Commun. Comput. Inf. Sci. 308 (2012) 797–803, http://dx.doi.org/10.1007/978-3-642-34041-3_110.

[7] J.S. Lim, Finding features for real time premature ventricular contraction detection using a fuzzy neural network system, IEEE Trans. Neural Networks 20 (2009) 522–527, http://dx.doi.org/10.1109/TNN.2008.2012031.

[8] L.Y. Shyu, Y.H. Wu, W. Hu, Using wavelet transform and fuzzy neural network for VPC detection form the Holter ECG, IEEE Trans. Biomed. Eng. 51 (2004) 1269–1273, http://dx.doi.org/10.1109/TBME.2004.824131.

[9] S. Poungponsri, X.H. Yu, An adaptive filtering approach for electrocardiogram (ECG) signal noise reduction using neural networks, J. Neurocomput. 117 (2013) 206–213, http://dx.doi.org/10.1016/j.neucom.2013.02.010.

[10] Y. Ozbay, R. Ceylan, B. Karlik, Integration of type-2 fuzzy clustering and wavelet transform in a neural network based ECG classifier, J. Expert Syst. Appl. 38 (2011) 1004–1010, http://dx.doi.org/10.1016/j.eswa.2010.07.118.

[11] B. Tighiouart, P. Rubel, M. Bedda, Improvement of QRS boundary recognition by means of unsupervised learning, IEEE comput. Soc. Press 30 (2003) 49–52, http://dx.doi.org/10.1109/CIC.2003.1291087.

[12] H.G. Rodney Tan, M. LumK, V.H. Mok, Performance evaluation of coifman wavelet for ECG signal denoising, Int. Feder. Med. Biol. Eng. 15 (2007) 419–422.

[13] Z. Lu, D.Y. Kim, W.A. Pearlman, Wavelet compression of ECG signals by the set artitioning in hierarchical trees algorithm, IEEE Trans. Biomed. Eng. 47 (2000) 849–856, http://dx.doi.org/10.1109/10.846678.

[14] H. Hassanpour, A. Parsaei, Fetal ECG extraction using wavelet transform, IEEE Comput. Intell. Model., Control Automation (2006) 179, http://dx.doi.org/10.1109/CIMCA.2006.98.

[15] F.A. Afsar, M. Afsar, Robust electrocardiogram (ECG) beat classification using discrete wavelet transform, IEEE Int. Conf. Bioinfor. Biomed. Eng. 2 (2008) 1867–1870, http://dx.doi.org/10.1109/ICBBE.2008.796.

[16] C.X. Zheng, C.W. Li, Detection of ECG characteristics points using the wavelet transforms, IEEE Trans. Biomed. Eng. 42 (1995) 21–28, http://dx.doi.org/10.1109/10.362922.

[17] N. Nikolaev, Z. Nikolov, A. Gotchev, K. Egiazarian, Wavelet domain Wiener filtering for ECG denoising using improved signal estimate, IEEE, Acoustics, Speech, Signal Process. 6 (2000) 3578–3581, http://dx.doi.org/10.1109/ICASSP.2000.860175.

[18] R. Benzid, F. Marir, A. Boussaad, M. Benyoucef, D. Arar, Fixed percentage of wavelet coefficients to be zeroed for ECG compression, IEEE Electronics Lett. 39 (2003) 830–831, http://dx.doi.org/10.1049/el:20030560.

[19] I. Nouira, A.B. Abdallah, M.H. Bedoui, M. Dogui, A robust R peak detection algorithm using wavelet transform for heart rate variability studies, Int. J. Elect. Eng. Infor. 5 (2013) 270–284, http://dx.doi.org/10.12691/bse-2-1-3.

[20] J.S. Sahambi, S.M. Tandon, R.K.P. Bhatt, Using wavelet transform for ECG characterization, IEEE Eng. Med. Biol. 16 (1997) 77–83, http://dx.doi.org/10.1109/51.566158.

[21] J.S. Sahambi, S.M. Tandon, R.K.P. Bhatt, Quantitative analysis of errors due to power-line interference and base-line drift in detection of onsets and offsets in ECG using wavelets, Med. Biol. Eng. Comput. 35 (1997) 747–751, http://dx.doi.org/10.1007/BF02510988.

[22] C. Li, C. Zheng, C. Tai, Detection of ECG characteristics points using wavelet transforms, IEEE Trans. Biomed. Eng. 42 (1995) 21–28, http://dx.doi.org/10.1109/10.362922.

[23] B. Gramatikov, J. Brinker, S. Yi-chun, N.V. Thakor, Wavelet analysis and time-frequency distributions of the body surface ECG before and after angioplasty, Comput. Methods Programs Biomed. 62 (2000) 87–98, http://dx.doi.org/10.1016/S0169-2607(00)00060-2.

[24] C. Li, C. Zheng, C. Tai, Detection of ECG characterictic points using wavelet transforms, IEEE Trans. Biomed. Eng. 42 (1995) 21–28, http://dx.doi.org/10.1109/10.362922.

[25] T.H. Linh, S. Osowski, M. Stodolski, On-line heart beat recognition using Hermite polynomials and neuro-fuzzy network, IEEE Trans. Instrum. Meas. 52 (2003) 1224–1231, http://dx.doi.org/10.1109/TIM.2003.816841.

[26] A. Link, P. Endt, M. Oeff, L. Trahms, Variability of the QRS in high resolution electrocardiograms and magnetocardiograms, IEEE Trans. Biomed. Eng. 48 (2001) 133–142, http://dx.doi.org/10.1109/10.909634.

[27] L. Gang, Y. Wenyer, L. Ling, An artificial intelligence approach to ECG analysis, IEEE Eng. Med. Biol. Mag. 19 (2000) 95–100, http://dx.doi.org/10.1109/51.827412.

[28] T. Ince, S. Kiranyaz, M. Gabbouj, A generic and robust system for automated patient-specific classification of ECG signals, IEEE Trans. Biomed. Eng. 56 (2009) 1415–1426, http://dx.doi.org/10.1109/TBME.2009.2013934.

[29] M. Kei-ichiro, H. Nakajima, T. Toyoshima, Real-time discrimination of ventricular tachyarrhythmia with fourier-transform neural network, IEEE Trans. Biomed. Eng. 46 (1999) 179–185, http://dx.doi.org/10.1109/10.740880.

[30] N. Dib, R. Benali, Z.H. Slimane, F.B. Reguig, Delineation of the complex QRS and the t-end using wavelet transform and surface indicator, IEEE Int. Workshop Syst., Signal Process. Applic. (2011) 83–86, http://dx.doi.org/10.1109/WOSSPA.2011.5931419.

[31] C. Weng, Classification of ECG complexes using self-organizing CMAC, Measurement 42 (2009) 399–407, http://dx.doi.org/10.1016/j.measurement.2008.08.004.

[32] J.L. Williams, E. Lesaffre, Comparison of multi-group logistic and linear discriminant ECG and VCG classification, J. Electrocardiol. 20 (1987) 83–92, http://dx.doi.org/10.1016/S0022-0736(87)80096-1.

[33] J. Pan, W.J. Tompkins, A real-time QRS detection algorithm, IEEE Trans. Biomed. Eng. 32 (1985) 230–236, http://dx.doi.org/10.1109/TBME.1985.325532.

[34] R. Poli, S. Cagnoni, G. Valli, Genetic design of optimum linear and nonlinear QRS detectors, IEEE Trans. Biomed. Eng. 42 (1995) 1137–1141, http://dx.doi.org/10.1109/10.469381.

[35] B. Giovanni, B. Christian, F. Sergio, Possibilities of using neural networks for ECG classification, J. Electrocardiol. 29 (1996) 10–16, http://dx.doi.org/10.1016/S0022-0736(96)80003-3.

[36] D.A. Coast, R.M. Stern, G.G. Cano, S.A. Briller, An approach to cardiac arrhythmia analysis using hidden Markov models, IEEE Trans. Biomed. Eng. 37 (1990) 826–836, http://dx.doi.org/10.1109/10.58593.

[37] T. Olmez, Classification of ECG waveforms using RCE neural network and genetic algorithm, Electron. Lett. 33 (1997) 1561–1562, http://dx.doi.org/10.1049/el:19971019.

[38] S. Osowski, T.H. Linh, ECG beat recognition using fuzzy hybrid neural network, IEEE Trans. Biomed. Eng. 48 (2001) 1265–1271, http://dx.doi.org/10.1109/10.959322.

[39] (a) S. Rosaria, M. Carlo, Artificial neural networks for automatic ECG analysis, IEEE Trans. Signal Process. 46 (1998) 1417–1425, http://dx.doi.org/10.1109/78.668803;
(b) H.H. Szu, Neural network adaptive wavelets for signal representation and classification, Opt. Eng. 31 (1992) 1907–1916, http://dx.doi.org/10.1117/12.59918.

[40] I. Saini, QRS detection using K-Nearest Neighbor algorithm (KNN) and evaluation on standard ECG databases, J. Adv. Res. 4 (2012) 331–344, http://dx.doi.org/10.1016/j.jare.2012.05.007.

[41] R. Silipo, C. Marchesi, Artificial neural networks for automatic ECG analysis, IEEE Trans. Signal Process. 46 (1998) 1417–1425, http://dx.doi.org/10.1109/78.668803.

[42] S. Wei, Y. Wang, Y. Zuo, Wavelet neural networks robust control of farm transmission line deicing robot manipulators, Comput. Standards Interfaces 34 (2012) 327–333, http://dx.doi.org/10.1016/j.csi.2011.11.001.

[43] H.L. Wei, S.A. Billings, Y.F. Zhao, L.Z. Guo, An adaptive wavelet neural network for spatio-temporal system identification, Neural Netw. 23 (2010) 1286–1299, http://dx.doi.org/10.1016/j.neunet.2010.07.006.

[44] S. Barro, M. Fernandez, Classifying multi-channel ECG patterns with adaptive neural network, IEEE Eng. Med. Biol. Mag. 17 (1998) 45–55, http://dx.doi.org/10.1109/51.646221.

[45] R. Benali, M.A. Chikh, Neuro fuzzy classifier for cardiac arrythmias recognition, J. Theor. Appl. Inf. Technol. 5 (2009) 577–583.

[46] R. Benali, N. Dib, F.B. Reguig, Cardiac arrhythmia diagnosis using a neuro-fuzzy approach, J. Mech. Med. Biol. 10 (2010) 417–429, http://dx.doi.org/10.1142/S021951941000354X.

[47] R. Benali, F.B. Reguig, Z.H. Slimane, Automatic classification of heartbeats using wavelet neural network, J. Med. Syst. 36 (2012) 883–892, http://dx.doi.org/10.1007/s10916-010-9551-7.

[48] O. Wieben, V. Afonso, W. Tompkins, Classification of premature ventricular complexes using filter bank features, induction of decision trees and a fuzzy rule-based system, Med. Biol. Eng. Comput. 37 (1999) 560–565, http://dx.doi.org/10.1007/BF02513349.

[49] B.U. Kohler, C. Hennig, R. Orglmeister, The principles of software QRS detection, IEEE Eng. Med. Biol. Mag. 21 (2002) 42–57, http://dx.doi.org/10.1109/51.993193.

[50] R.W.D. Pedro, F.L.S. Nunes, A.M. Lima, Using grammars for pattern recognition in Images: A Systematic Review, ACM Comput. Survey 46 (2013) 1–34, http://dx.doi.org/10.1145/2543581.2543593.

[51] G. Kókai, J. Csirik, T. Gyimóthy, Learning the syntax and semantic rules of an ECG grammar, Lect. Notes Comput. Sci. 1321 (1997) 171–180, http://dx.doi.org/10.1007/3-540-63576-9_106.

[52] P. Trahanias, E. Skordalakis, Syntactic pattern recognition of the ECG, IEEE Trans. Pattern Anal. Mach. Intell. 12 (1990) 648–657, http://dx.doi.org/10.1109/34.56207.
[53] S. Hamdi, A.B. Abdallah, M.H. Bedoui, Grammar formalism for ECG signal interpretation and classification, Appl. Med. Inf. 35 (2014) 21–26.
[54] W.P. Holsinger, K.M. Kempner, M.H. Miller, A QRS preprocessor based on digital differentiation, IEEE Trans. Biomed. Eng. 18 (1971) 212–217, http://dx.doi.org/10.1109/TBME.1971.4502834.
[55] J. Fraden, M.R. Neumann, QRS wave detection, Med. Biol. Eng. Comput. 18 (1980) 125–132, http://dx.doi.org/10.1007/BF02443287.
[56] L.M. Hanieh, A.M. Fardin, F. Abdolhossein, A novel grammar-based approach to atrial fibrillation arrhythmia detection for pervasive healthcare environments, J. Comput. Security 2 (2015) 155–163.
[57] J. Gao, X. Ding, J. Zheng, Image pattern recognition based on examples-a combined statistical and structural-syntactic approach, Lect. Notes Comput. Sci. 1876 (2000) 57–66, http://dx.doi.org/10.1007/3-540-44522-6_6.
[58] J. Ayyoob, Sleep apnoea detection from ECG using features extracted from reconstructed phase space and frequency domai, Biomed. Signal Process. Control 8 (2013) 551–559, http://dx.doi.org/10.1016/j.bspc.2013.05.007.
[59] P.S. Hamilton, W.J. Tompkin, Quantitative investigation of QRS detection rules using MIT/BIH Arrhythmia database, IEEE IEEE Eng. Med. Biol. Magaz. 33 (1986) 1157–1165, http://dx.doi.org/10.1109/TBME.1986.325695.
[60] S.A. Chouakri, F.B. Reguig, A.T. Ahmed, QRS complex detection based on multiwavelet packet decomposition, Appl. Math. Comput. 217 (2011) 9508–9525, http://dx.doi.org/10.1016/j.amc.2011.03.001.
[61] Z.H. Slimane, N.A. Amine, QRS complex detection using empirical mode decomposition, Digital Signal Process. 20 (2010) 1221–1228, http://dx.doi.org/10.1016/j.dsp.2009.10.017.
[62] I. Christov, Real time electrocardiogram QRS detection using combined Adaptive Threshold, Biomed. Eng. Online 3 (2004) 28, http://dx.doi.org/10.1186/1475-925X-3-28.
[63] A. Ghaffari, H. Golbayani, M. Ghasemi, A new mathematical based QRS detector using continuous wavelet transform, Comput. Electr. Eng. 38 (2008) 81–91, http://dx.doi.org/10.1016/j.compeleceng.2007.10.005.
[64] A. Kyrkos, E.A. Giakoumakis, G. Carayannis, QRS detection through time recursive prediction technique, Signal Process. 15 (1988) 429–436, http://dx.doi.org/10.1016/0165-1684(88)90061-8.
[65] S.S. Mehta, N.S. Lingayat, Development of SVM based classification techniques for the Delineation of wave components in 12-lead electrocardiogram, Biomed. Signal Process. Control 3 (2008) 341–349, http://dx.doi.org/10.1016/j.bspc.2008.04.002.
[66] F. Gritzali, Towards a generalized scheme for QRS detection in ECG waveforms, Signal Process. 15 (1998) 183–192, http://dx.doi.org/10.1016/0165-1684(88)90069-2.
[67] P.E. Trahanias, An approach to QRS-complex detection using mathematical morphology, IEEE Trans. Biomed. Eng. 40 (1993) 201–205, http://dx.doi.org/10.1109/10.212060.

Salah Hamdi; Received his Ph.D degree in computer sciences from the National School of Engineering of Sfax (ENIS) in 2016, Tunisia. He had his Master degree in computer sciences from the Upper Institute of the Applied Sciences and Technology (ISSATS) in 2008, Tunisia. At present, he is a member of the Research laboratory of Technology and Medical Imaging (LTIM) at the Faculty of Medicine of Monastir (FMM). His current research topics focus on medical imaging and signals.

Asma Ben Abdallah; Received her Ph.D degree in computer sciences from the National School of computer Sciences (ENSI) in 2007, Tunisia. She had his HDR degree in computer sciences in 2016. Currently, she is member of the research Laboratory of Technology and Medical Imaging (LTIM) at the Faculty of Medicine of Monastir (FMM). Her current research topics focus on medical imaging and signals.

Mohamed Hedi Bedoui; Received his Ph.D degree in Genie Bio medical from University of Lille – France in 1992. Full Professor and Chairman of the Communication Committee and Resources of the Faculty of Medicine of Monastir (FMM), Tunisia. Leader of the Research laboratory of Technology and Medical Imaging (LTIM). Member of the French Society of Biological and Medical Engineering (SFGBM). President of the Tunisian Association for the Promotion of Applied Research (ATUPRA). His current interests include the conception of electronic and informatics systems used in the medical field.